Local rather than global H3K27me3 dynamics associates with differential gene expression in *Verticillium dahliae*

H. Martin Kramer[1], Michael F. Seidl[1,2], Bart P.H.J. Thomma[1,3,#,*], David E. Cook[1,4,*]

[1]Laboratory of Phytopathology, Wageningen University and Research, Droevendaalsesteeg 1, 6708 PB Wageningen, the Netherlands

[2]Theoretical Biology & Bioinformatics Group, Department of Biology, Utrecht University, Utrecht, The Netherlands

[3]University of Cologne, Institute for Plant Sciences, Cluster of Excellence on Plant Sciences (CEPLAS), 50674 Cologne, Germany

[4]Department of Plant Pathology, Kansas State University, 1712 Claflin Road, Manhattan, Kansas 66506, USA

[*]These authors contributed equally

[#]For correspondence: bthomma@uni-koeln.de

Running title: Global histone dynamics in *Verticillium dahliae*

Word count Abstract: 237

Word count Importance: 150

Word count text: 6.466

ABSTRACT

Differential growth conditions typically trigger global transcriptional responses in filamentous fungi. Such fungal responses to environmental cues involve epigenetic regulation, including chemical histone modifications. It has been proposed that conditionally expressed genes, such as those that encode secondary metabolites but also effectors in pathogenic species, are often associated with a specific histone modification, lysine27 methylation of H3 (H3K27me3). However, thus far no analyses on the global H3K27me3 profiles have been reported under differential growth conditions in order to assess if H3K27me3 dynamics governs differential transcriptional. Using ChIP- and RNA-sequencing data from the plant pathogenic fungus *Verticillium dahliae* grown on three *in vitro* cultivation media, we now show that a substantial number of the identified H3K27me3 domains globally display stable profiles among these growth conditions. However, we do observe local quantitative differences in H3K27me3 ChIP-seq signal that associate with differentially transcribed genes between media. Comparing the *in vitro* results to expression during plant infection suggests that *in planta* induced genes require chromatin remodelling to achieve expression. Overall, our results demonstrate that although some loci display H3K27me3 dynamics that can contribute to transcriptional variation, other loci do not show such dependence. Thus, we conclude that while H3K27me3 is required for transcriptional repression, it is not a conditionally responsive global regulator of differential transcription. We propose that the H3K27me3 domains that do not undergo dynamic methylation may contribute to transcription through other mechanisms or may serve additional genomic regulatory functions.

IMPORTANCE

In many organisms, including filamentous fungi, epigenetic mechanisms that involve chemical and physical modifications of DNA without changing the genetic sequence have been implicated in transcriptional responses upon developmental or environmental cues. In fungi, facultative heterochromatin that can de-condense to allow transcription in response to developmental changes or to environmental stimuli is characterized by tri-

methylation of lysine 27 on histone H3 (H3K27me3), and H3K27me3 has been implicated in transcriptional regulation although precise mechanisms and functions remain enigmatic. Based on ChIP- and RNA-sequencing data, we show for the soil-borne broad host range vascular wilt plant pathogenic fungus *Verticillium dahliae* that although some loci display H3K27me3 dynamics that can contribute to transcriptional variation, other loci do not show such dependence. Thus, although we recognize that H3K27me3 is required for transcriptional repression, we also conclude that this mark is not a conditionally responsive global regulator of differential transcription upon responses to environmental cues.

60 **INTRODUCTION**

61 The fungal kingdom comprises a plethora of species occupying an enormously diverse
62 range of ecological niches (Schmit & Mueller, 2007). As environments are typically
63 dynamic, including the effects of daily and yearly cycles, fungi continuously need to
64 respond and adapt to survive (Gibson, 2008; Selvig & Alspaugh, 2011). To this end,
65 fungi have evolved various mechanisms to monitor their environment and to
66 transcriptionally respond to environmental cues (Bahn *et al.*, 2007). For instance, the
67 yeast *Saccharomyces cerevisiae* senses cold stress by increased membrane rigidity,
68 which leads to transcription of genes that, among others, encode cell damage-preventing
69 proteins (Aguilera *et al.*, 2007). Furthermore, *S. cerevisiae* senses the quantitative
70 availability of carbon and nitrogen sources in the environment to determine which
71 developmental program maximises the potential for survival (Schneper *et al.*, 2004). In
72 animal systems, epigenetic mechanisms (i.e. those affecting nuclear processes by
73 modifying DNA characteristics without changing the genetic sequence) are implicated in
74 transcriptional responses to changing environments (Heijmans *et al.*, 2008; Zannas *et*
75 *al.*, 2015; Martin & Fry, 2018). Such epigenetic mechanisms have similarly been
76 proposed to contribute to environmental response in filamentous fungi. For instance, the
77 saprotrophic fungus *Neurospora crassa* phenotypically reacts to environmental stimuli,
78 such as changes in temperature and pH, yet *N. crassa* mutants impaired in transcription-
79 associated epigenetic mechanisms display reduced growth in response to these stimuli
80 (Kronholm *et al.*, 2016). Similarly, the nectar-feeding yeast *Metschnikowia reukaufii* and
81 the ubiquitous fungus *Aureobasidium pullulans* fail to properly respond to changing
82 carbon sources when DNA methylation or histone acetylation are inhibited (Slepecky &
83 Starmer, 2009; Herrera *et al.*, 2012). These results suggest that epigenetic mechanisms
84 are important for transcriptional responses to changing environments in diverse fungi,
85 but many questions remain regarding the precise mechanisms and function of epigenetic
86 dynamics in fungi.

87 Epigenetic mechanisms, such as direct modifications of DNA and histone proteins
88 or physical changes to the chromatin architecture, can influence transcription by

89 regulating DNA accessibility (Slotkin & Martienssen, 2007). Chromatin that is accessible
90 and potentially active is termed euchromatin, while heterochromatin is condensed and
91 often transcriptionally silent (Bannister & Kouzarides, 2011). However, heterochromatic
92 regions are not always repressed. Heterochromatin is subcategorized into constitutive
93 heterochromatin that remains condensed throughout the cell cycle, and facultative
94 heterochromatin that can de-condense to allow transcription in response to
95 developmental changes or to environmental stimuli (Trojer & Reinberg, 2007; Kim *et al.*,
96 2015; Wang *et al.*, 2016). In fungi, constitutive heterochromatin is often associated with
97 repeat-rich genome regions and is typically characterized by tri-methylation of lysine 9
98 on histone H3 (H3K9me3), while facultative heterochromatin is characterized by tri-
99 methylation of lysine 27 on histone H3 (H3K27me3) (Lewis *et al.*, 2009, 2010; Jamieson
100 *et al.*, 2013; Freitag, 2017). Empirically, both H3K9me3 and H3K27me3 have been
101 implicated in transcriptional regulation in various fungi (Reyes-Dominguez *et al.*, 2010,
102 2012; Connolly *et al.*, 2013; Wiemann *et al.*, 2013; Chujo & Scott, 2014; Soyer *et al.*,
103 2014). The majority of these studies rely on genetic perturbation of the enzymes that
104 deposit methylation at H3K9 and H3K27, and the results consistently show that depletion
105 of methylation at these lysine residues mainly results in transcriptional induction.
106 However, as global depletion of a histone modification can result in pleiotropic effects,
107 such as improper localization of other histone modifications or altered development (Tian
108 & Chen, 2001; Fan *et al.*, 2017), it is difficult to infer transcriptional control mechanisms
109 used for natural gene regulation from these genetic perturbation experiments. Therefore,
110 additional research is needed to directly test the hypothesis that heterochromatin-
111 associated histone modifications directly regulate transcription either through their
112 dynamics, or their action to form or recruit transcriptional complexes (Galazka & Freitag,
113 2014; Seidl *et al.*, 2016; Ridenour *et al.*, 2020).

114 The filamentous fungus *Verticillium dahliae* is a soil-borne broad host-range plant
115 pathogen that infects plants through the roots to invade the xylem vessels and cause
116 vascular wilt disease (Fradin & Thomma, 2006). Genomic and transcriptomic studies
117 have revealed that the *V. dahliae* genome harbours lineage-specific (LS) regions that are

118 variable between strains and enriched for genes that are *in planta* induced (Klosterman
119 *et al.*, 2011; de Jonge *et al.*, 2013). These LS regions are generally considered genomic
120 hotspots for evolutionary adaptation to plant hosts (Klosterman *et al.*, 2011; de Jonge *et*
121 *al.*, 2013; Faino *et al.*, 2016; Shi-Kunne *et al.*, 2018; Depotter *et al.*, 2019; Cook *et al.*,
122 2020). Recently we explored the epigenome of *V. dahliae* and distinguished LS regions
123 from the core genome based on particular chromatin signatures, including elevated levels
124 of H3K27me3 accompanied with accessible DNA and active transcription (Cook *et al.*,
125 2020). Using a machine learning approach and supported by orthogonal analyses, we
126 identified nearly twice as much LS DNA as previously considered, collectively referred to
127 as adaptive genomic regions (Cook *et al.*, 2020). Given the elevated levels of H3K27me3
128 at adaptive genomic regions in *V. dahliae*, and previous reports that removal of
129 H3K27me3 results in transcriptional induction (Connolly *et al.*, 2013; Chujo & Scott,
130 2014; Soyer *et al.*, 2014), we now tested if H3K27me3 dynamics are required for
131 transcriptional activation of genes in adaptive genomic regions. Ideally, the involvement
132 of H3K27me3 dynamics in differential gene expression of *V. dahliae* would be studied
133 between *in vitro* and *in planta* growth, as adaptive genomic regions are enriched for *in*
134 *planta* induced genes (de Jonge *et al.*, 2013; Cook *et al.*, 2020). However, *V. dahliae*
135 displays a low pathogen-to-plant biomass during infection (Faino *et al.*, 2012), which
136 impedes technical procedures to determine histone modification levels over the genome
137 (Soyer *et al.*, 2015). Nevertheless, as H3K27me3 is generally reported to regulate
138 transcription in response to environmental stimuli (Trojer & Reinberg, 2007; Wang *et al.*,
139 2016), we hypothesize that it may be involved in transcriptional regulation in *V. dahliae*
140 during differential growth conditions *ex planta* as well. Here, we analyse RNA-seq, ChIP-
141 seq and ATAC-seq data of *V. dahliae* cultured in various axenic growth media to
142 understand if transcriptional dynamics require concomitant changes in the H3K27me3
143 modification status.
144

145 **RESULTS**

146 **Genes induced between growth conditions are associated with H3K27me3**

147 We sought to test if genes in adaptive genomic regions, which we recently reported to
148 have distinct chromatin profiles (Cook *et al.*, 2020), are transcriptionally more responsive
149 to differential *in vitro* and *in planta* growth conditions. We found that genes that are
150 higher expressed in Czapec-Dox (CZA) or Murashige-Skoog (MS) media when compared
151 with potato dextrose broth (PDB) are significantly enriched in adaptive genomic regions
152 (two-sided two-proportions Z-test, $p<0.01$) (Fig. 1A). More specifically, 125 (14.6%) out
153 of 856, and 84 (11.8%) out of 711 genes that are higher expressed in CZA or MS than in
154 PDB, respectively, locate in adaptive genomic regions, while these regions only comprise
155 998 (8.7%) of the total 11,426 genes in the genome (two-sided two-proportions Z-test,
156 $p<0.01$) (Fig. 1A). Interestingly, genes with greater transcriptional differences between
157 the media (i.e. higher $\log_2$-fold changes) appear to be increasingly more overrepresented
158 in adaptive genomic regions than those with smaller or no differences (Fig. 1A).

159 We next compared expression during infection of *Arabidopsis thaliana* to
160 cultivation in PDB. We found that genes that are higher expressed during *A. thaliana*
161 colonization are also overrepresented in adaptive genomic regions, consistent with other
162 host-infection experiments for *V. dahliae* (de Jonge *et al.*, 2013; Cook *et al.*, 2020).
163 Similar to what we observed for *in vitro* growth conditions, genes with the greatest
164 transcriptional dynamics are increasingly more overrepresented in adaptive genomic
165 regions. That is, there are 145 (14.7%) out of 987 genes higher expressed *in planta*
166 ($\log_2$-fold change >2) residing in adaptive genomic regions, while at $\log_2$-fold change >7
167 this increases to 26 (36.6%) out of 71 (Fig. 1A). These results show that genes higher
168 expressed in other *in vitro* growth media compared to PDB, as well as genes that are
169 higher expressed during plant infection compared to PDB, are overrepresented in
170 adaptive genomic regions. Thus, these data suggest that genes that respond to
171 environmental cues in general, rather than only genes that are induced *in planta*, are
172 overrepresented at adaptive genomic regions.

173 Given the elevated levels of H3K27me3 at adaptive genomic regions in *V. dahliae*
174 (Cook *et al.*, 2020), one potential explanation for the co-localization of genes that are
175 differentially expressed *in vitro* and those that are differentially expressed *in planta* is

176 that these responses to different growth conditions share an adaptive origin that is
177 epigenetically regulated by H3K27me3. However, given that H3K27me3 occurs not only
178 in adaptive genomic regions in *V. dahliae*, but also throughout the core genome (Cook *et*
179 *al.*, 2020), we sought to determine if H3K27me3 is associated with *in vitro* and *in planta*
180 differentially expressed genes, not only in adaptive genomic regions, but also genome-
181 wide. Thus, we first performed peak calling on H3K27me3-ChIP data of *V. dahliae*
182 cultivated for 6 days in PDB and obtained 304 H3K27me3 domains that cover
183 approximately 10.5 Mb (28.9%) of the genome (Fig. S1), comprising 3,280 (28.7%)
184 genes and overlapping 87.4% of adaptive genomic regions. Interestingly, the observed
185 overrepresentation of differentially expressed genes in the generally H3K27me3-marked
186 adaptive genomic regions extends to H3K27me3 domains throughout the genome,
187 showing that H3K27me3 is genome-wide associated with differentially expressed genes
188 (Fig. 1B). Specifically, when assessing what fraction of higher expressed genes in CZA,
189 MS or Arabidopsis when compared with PDB locate in an H3K27me3 domain, we found
190 that 421 (49.2%) out of 856, 271 (38.1%) out of 711, and 453 (45.9%) out of 987
191 locate in H3K27me3 domains, respectively (Fig. 1B, $\log_2$-fold change >2), which is
192 considerably more than the 28.7% genome-wide average. Additionally, similar to our
193 observations for adaptive genomic regions, we also observed that genes displaying
194 higher $\log_2$-fold changes were increasingly overrepresented in H3K27me3 domains. Here
195 we found that 41 out of 51 (80.4%), 4 out of 7 (57.1%), and 54 out of 71 (76.0%)
196 genes higher expressed with a $\log_2$-fold change >7 in CZA, MS and Arabidopsis,
197 respectively, located in H3K27me3 domains (Fig. 1B). Collectively, these data reveal a
198 strong association between differential gene expression and the presence of H3K27me3
199 domains, both for genes that are differentially expressed between *in vitro* growth
200 conditions, as well as for genes that are higher expressed *in planta* than *in vitro.* As we
201 observed that the association with differentially expressed genes is not limited to
202 adaptive genomic regions, but is a feature for H3K27me3 domains in general, we infer
203 that H3K27me3 may be involved in regulating transcriptional changes in response to
204 environmental cues.

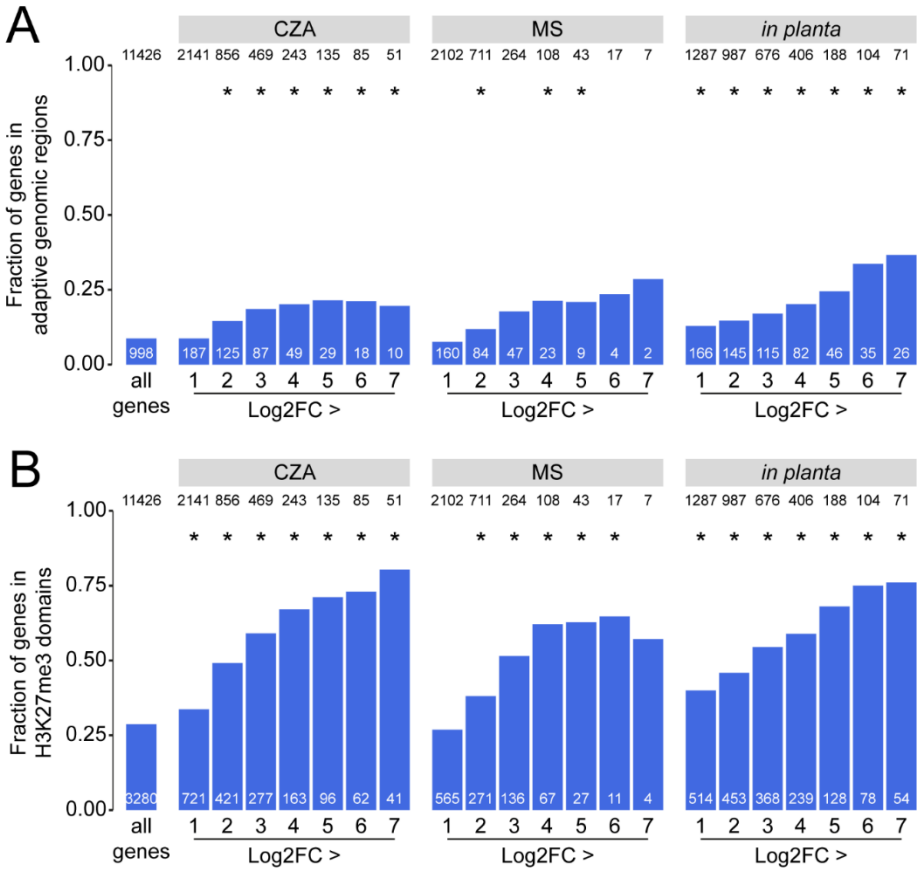

Figure 1. Genes that are higher expressed in CZA, MS and *in planta* than in PDB are overrepresented in adaptive genomic regions and in H3K27me3 domains. Fractions of total genes and genes that are higher expressed than in PDB that locate in (A) adaptive genomic regions and (B) H3K27me3-enriched regions. Increased expression is determined between six days of cultivation *in vitro* of *V. dahliae* in potato dextrose broth (PDB) and 6 days of cultivation in Czapec-Dox (CZA) and half-strength Murashige Skoog medium (MS), and infection of *Arabidopsis thaliana* (21 dpi) (*in planta*). Fractions of higher expressed genes that reside in adaptive genomic regions or H3K27me3-enriched regions are reported for log2-fold changes >1, 2, 3, 4, 5, 6 and 7, respectively. H3K27me3-enrichment was determined for *V. dahliae* cultivation during six days in PDB. Black numbers above the bars indicate numbers of genes per gene set. White numbers at bottom of the bars indicate the numbers of genes that locate in adaptive genomic or H3K27me3-domain per gene set. Significance of fraction differences was calculated for each fraction of higher expressed genes in adaptive genomic regions when compared with the fraction of total genes in adaptive genomic regions, by the two-sided two-proportions Z-test (*: $p \leq 0.05$).

Chromatin features correlate with gene expression levels

To generally assess how chromatin impacts transcriptional activity in *V. dahliae*, we determined the occurrence of the heterochromatic histone mark H3K9me3, the euchromatic histone mark H3K4me2, and chromatin accessibility determined by assay for transposase accessible chromatin followed by sequencing (ATAC-seq) (Buenrostro *et al.*, 2015). Grouping the *V. dahliae* genes into five expression quintiles, from quintile 1 containing the highest 20% expressed genes to quintile 5 with the 20% lowest expressed

227 genes, we are able to integrate histone modification profiles and transcriptional activity.
228 Expressed genes (quintiles 1-4) displayed low H3K4me2 coverage upstream of the
229 transcription start site (TSS), followed by a steep increase of coverage over the start of
230 the gene that decreases over the gene body (Fig. 2B). The strength of the association
231 corresponds to the level of transcription, also within quintiles (Fig. S2). The low
232 H3K4me2 coverage near the TSS coincides with increased chromatin accessibility, where
233 higher expressed quintiles have more open DNA (Fig. 2B, Fig. S2). There is little evidence
234 of H3K9me3 over gene bodies and *cis*-regulatory regions (Fig. 2B, Fig. S2), which
235 corroborates that H3K9me3 marks TEs in constitutive heterochromatic regions such as
236 the centromeres (Lewis *et al.*, 2009; Schotanus *et al.*, 2015; Cook *et al.*, 2020; Seidl *et*
237 *al.*, 2020). During cultivation in PDB, H3K27me3 is mainly present on genes that are
238 lowly or not expressed (quintile 4 and 5) (Fig. 2B, Fig. S2). Collectively, this empirical
239 description of chromatin and transcriptional activity is consistent with reports for other
240 fungi (Reyes-Dominguez *et al.*, 2010; Connolly *et al.*, 2013; Möller *et al.*, 2019).

241 To further analyse the association between H3K27me3 and gene expression, we
242 generated expression quintiles for the genes located in H3K27me3 domains during PDB
243 growth (3,280 genes). Interestingly, we found that genes in this group with higher
244 expression values (e.g. quintile 1 and 2) had higher H3K4me2 over the gene body, more
245 accessible promoters, and lower H3K27me3 values (Fig. 2C). This suggests that genes in
246 H3K27me3 domains are not uniformly repressed or heterochromatic, and there appeared
247 to be a quantitative, rather than qualitative association between H3K27me3 association
248 and gene activity. Genes with a lower association to H3K27me3 may represent loci that
249 are not in a stable state under the tested conditions, where some cells have a more
250 euchromatic profile and other have a more heterochromatic profile. While we cannot infer
251 these details from the current data, it is clear that genes with lower expression in PDB
252 are generally marked with H3K27me3, have less H3K4me3 and have less accessible DNA
253 in the region of transcription initiation (i.e. their promoter).

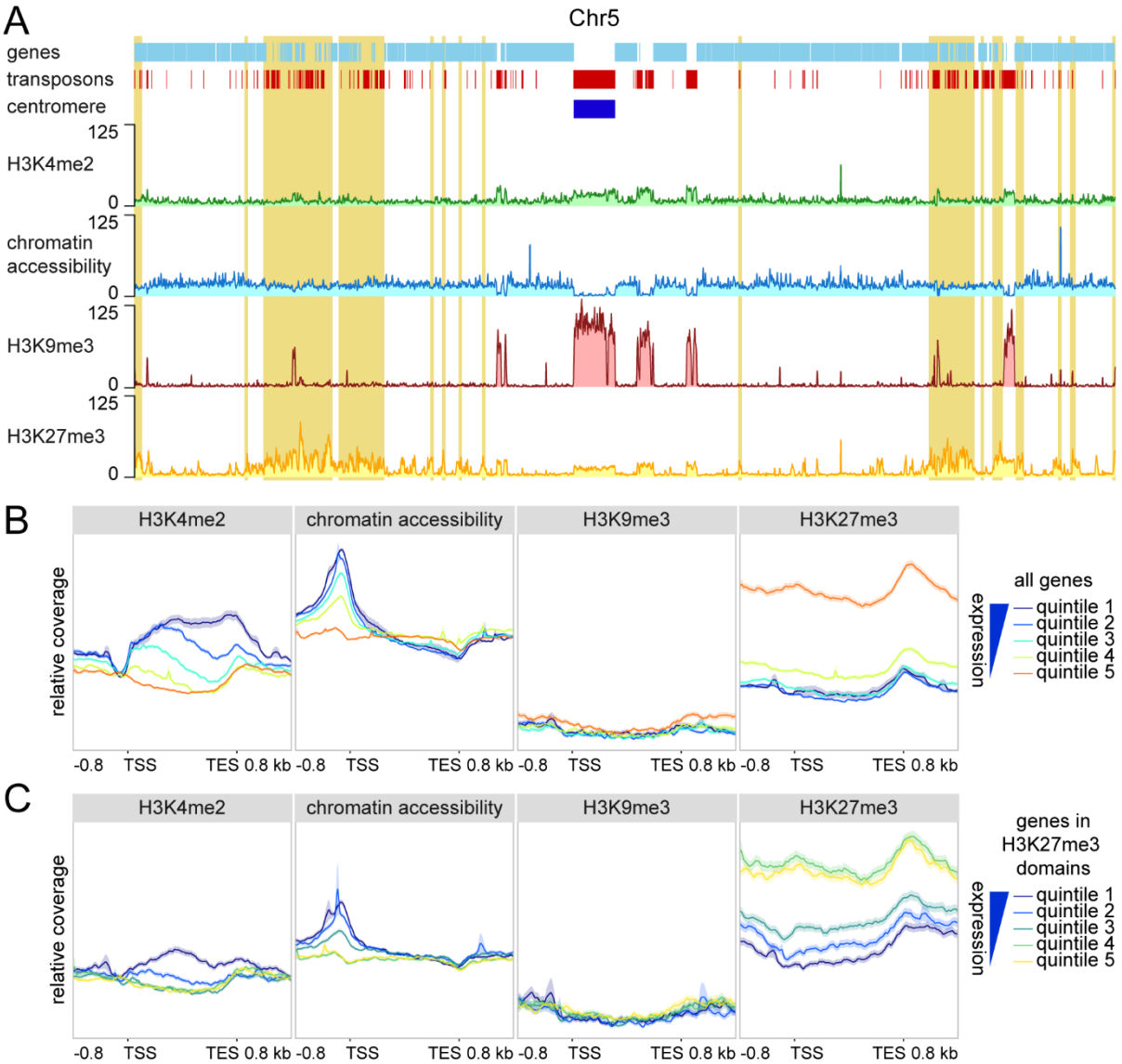

Figure 2. Lowly and non-expressed genes associate with H3K27me3. A) Whole genome distribution of the euchromatin-associated histone modification H3K4me2, the constitutive heterochromatin-associated histone modification H3K9me3, the facultative heterochromatin-associated histone modification H3K27me3 and chromatin accessibility as determined by ATAC-seq, based on chromosome 5 as an example. Genes are indicated in light blue, transposons are indicated in red, centromere is indicated in dark blue and adaptive genomic regions are indicated in yellow. B,C) Relative coverage of chromatin accessibility and the histone marks H3K4me2, H3K9me3, H3K27me3 over gene bodies (between transcription start site (TSS) and transcription end site (TES)) ±800 bp of flanking sequence, grouped into quintiles based on gene expression levels upon cultivation for six days potato dextrose broth (PDB), for (B) all genes, and for (C) all H3K27me3-enriched genes.

Genetic perturbation of H3K27me3 induces transcription of many genes that are differentially expressed *in vitro* and *in planta*

To further characterize the influence of H3K27me3 on gene expression in *V. dahliae*, we deleted the histone methyltransferase component of the Polycomb Repressive Complex 2 (PRC2), termed *Set7* (Δ*Set7*), leading to loss of H3K27me3 (Fig. S3). As H3K27me3 is

271 generally associated with facultative heterochromatin, we anticipated that the loss of
272 H3K27me3 would mainly lead to induction of genes that were located in H3K27me3
273 domains in wild-type *V. dahliae*. Out of the 839 genes that are induced in Δ*Set7* (log_2-
274 fold change >2, $p<0.05$), 615 (73.3%) locate in H3K27me3 domains, which is
275 significantly higher than expected given that only 28.7% of genes locate in H3K27me3
276 domains (Fisher's exact test, $p<0.00001$). In contrast, we find that 214 (28.0%) of 765
277 repressed genes in Δ*Set7* are in H3K27me3 domains (no association, Fisher's exact test,
278 $p=0.78$) (Fig. 3A,B). Additionally, when comparing log_2-fold changes in expression
279 between Δ*Set7* and the wild type strain, we observed that genes located in a H3K27me3
280 domain in wild type are more significantly induced in Δ*Set7* than genes not locating in
281 H3K27me3 domains (Two-sample Student's T-test, $p<0.001$) (Fig. S4). These findings
282 suggest that H3K27me3 represses transcription at marked regions.

283 We next sought to integrate the repressive transcriptional effects of H3K27me3
284 inferred from Δ*Set7* RNA-seq with the differential transcription observed between growth
285 conditions. For this, we compared genes induced in Δ*Set7* versus wild-type PDB growth
286 with genes higher expressed in CZA, MS or *in planta* versus PDB growth. There is a
287 significant overrepresentation of genes induced in Δ*Set7* (839), and those induced in CZA
288 (254 genes, 30.3% overlap, Fisher's exact test $p<0.00001$), MS (197 genes, 23.5%
289 overlap, Fisher's exact test $p<0.00001$) and *in planta* (208 genes, 24.8% overlap,
290 Fisher's exact test $p<0.00001$). These associations are higher than the background levels
291 of genes induced under CZA, MS or *in planta*, which is 7.5%, 6.2%, and 8.6% of genes,
292 respectively (Fig. 3C-E). Together, these data show that H3K27me3 is required for
293 transcriptional silencing of mainly H3K27me3 associated genes, and that many of these
294 genes are also differentially expressed between the tested growth conditions. These
295 results support the hypothesis that transcriptional dynamics between the tested growth
296 conditions are regulated, at least partly, by levels of H3K27me3.

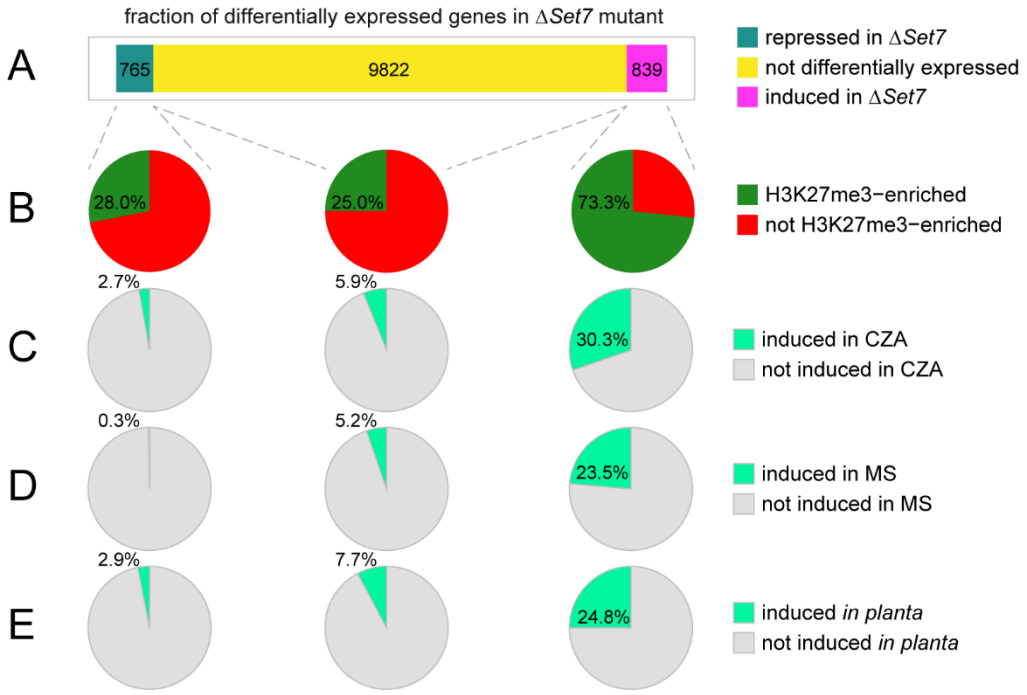

Figure 3. Genetic perturbation of H3K27me3 results in induction of genes that are transcriptionally regulated in different growth conditions. A) Fractions of induced (log2 fold change >1, p<0.05) and repressed (log2 fold change <-1, p<0.05) genes and genes that are not differentially expressed between wild-type and ΔSet7 that (B) locate in H3K27me3 domains and (C-E) are higher expressed in CZA, MS and *in planta* than in PDB.

H3K27me3 domains are globally stable between *in vitro* growth conditions

Under the hypothesis that H3K27me3 dynamics contribute to differential gene expression, we predict that H3K27me3 ChIP-seq domains will change when *V. dahliae* is grown under different conditions. In addition, the observed changes in H3K27me3 domains will be associated with transcriptional differences of the underlying genes. To test this hypothesis, we performed additional H3K27me3 ChIP-seq for *V. dahliae* cultured in MS and CZA, and identified H3K27me3 domains from replicate H3K27me3 ChIP-seq in each of the three growth media. We identified a total of 1,631 genes that were always present in H3K27me3 domains, regardless of the *in vitro* growth media (Fig. 4A). Not surprisingly, the 1,631 genes present in stable H3K27me3 domains were significantly lower expressed when compared with non-marked genes in all three growth conditions (Fig. 4B). To assess if changes in H3K27me3 domains between the media were associated with changes in transcription, we compared domains and gene expression between media. We first analysed RNA-seq output for genes present in H3K27me3

317 domains in two media but not in an H3K27me3 domain in the third medium. For
318 example, we identified 703 genes that were in a H3K27me3 domain in PDB and in MS but
319 not in CZA (Fig. 4A), and found that these genes were more highly expressed during CZA
320 growth when compared with growth in PDB or in MS (Fig. 4C). These result corroborated
321 the association between the lack of H3K27me3 in CZA and increased transcription of the
322 underlying genes. However, genes present in shared H3K27me3 domains for MS and CZA
323 growth (229), or CZA and PDB growth (44) did not display statistically significant
324 transcriptional differences between the growth conditions where the genes lack
325 H3K27me3 domains (Fig. 4A, C). Analysing H3K27me3 domains unique to a media, we
326 found that MS growth had the greatest number and proportion of unique genes locating
327 in H3K27me3 domains (18.3%), followed by 12.4% unique to CZA growth, and 4.7%
328 unique to PDB growth (Fig. 4A). The genes uniquely marked in PDB had a non-
329 significant, but lower median expression value when compared with the other two media.
330 Genes uniquely located in MS H3K27me3 domains were significantly lower expressed
331 when compared with growth in CZA, but not with growth in PDB (Fig. 4D). The genes
332 uniquely present in CZA H3K27me3 domains did not display transcriptional differences
333 when *V. dahliae* was grown in the other two media. Overall, these results show that
334 H3K27me3 contributes to transcriptional repression, but there is not a simple global
335 association between H3K27me3 presence/absence dynamics and transcriptional output.
336 We observed clear examples where the loss of H3K27me3 in one medium is associated
337 with increased transcription in that medium, but this is not ubiquitous. We note that the
338 majority of genes located in H3K27me3 domains were common to all three growth
339 conditions, accounting for 75%, 65.4% and 52% of the identified genes in H3K27me3
340 domains from CZA, PDB, and MS growth, respectively, indicating that the qualitative
341 presence of H3K27me3 domains is globally stable.

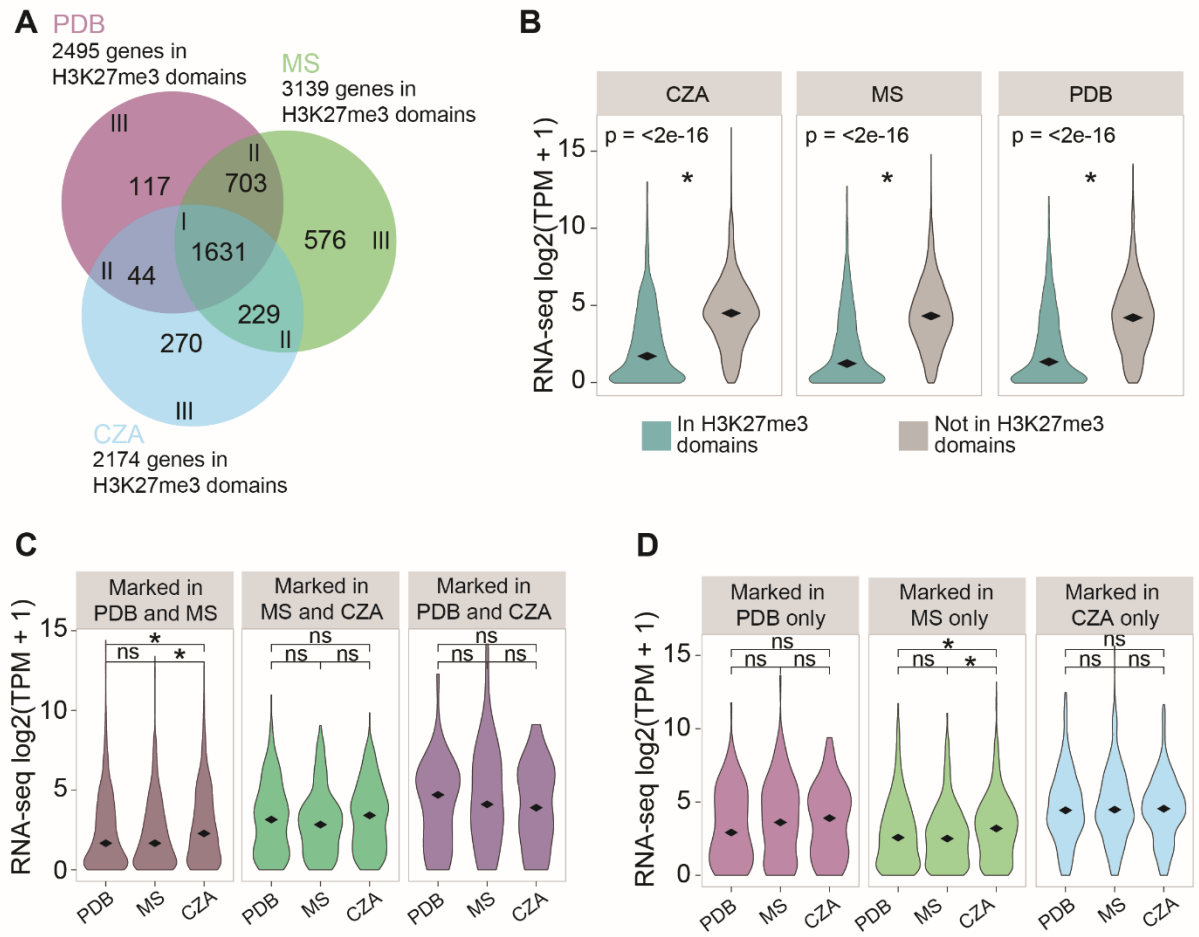

Figure 4. Differential H3K27 methylation partially explains differential expression. A) The number of genes located in H3K27me3 domains for *V. dahliae* cultivated for 6 days in Czapec-Dox (CZA), half-strength Murashige Skoog medium (MS) and Potato dextrose broth (PDB). B) Transcriptional values from RNA-seq, represented as TPM values in each growth medium. The genes were grouped between those consistently localized in H3K27me3 domains (1631 genes) and genes not present in H3K27me3 domains. C,D) Transcription TPM values in each growth medium for genes in H3K27me3 domains found in C) two or D) one of three tested *in vitro* growth media. Median values of violin plots are indicated with diamonds. Significant difference of TPM values between growth media are determined with the One-Sample Wilcoxon Signed Rank Test (*: p <= 0.05).

Local quantitative differences in H3K27me3 levels are associated with transcriptional differences

Our analysis on H3K27me3 presence/absence dynamics did not account for potential quantitative differences between growth media. Whole chromosome plots of H3K27me3 domains identified between media reflect their generally stable presence (Fig. S5A), but the quantitative level of ChIP-seq signal appeared to vary at some loci within called domains (Fig. S5B). To address this, we examined quantitative differences between H3K27me3 ChIP-seq signal and transcriptional output between pairs of growth conditions. Genes were grouped based on differential gene expression between media,

361 where genes higher expressed in medium A were one group and genes higher expressed
362 in medium B another group. The H3K27me3 ChIP-seq levels were compared between the
363 groups for the ChIP conducted in both the transcriptionally permissive and non-
364 permissive growth conditions. Comparing results for PDB versus MS, we see that genes
365 higher expressed in MS have a significantly lower H3K27me3 signal from MS-ChIP versus
366 the same genes from PDB-ChIP (Fig. 5A). For genes more highly expressed in PDB, there
367 is a higher, but not significantly different, H3K27me3 ChIP-seq level when grown in MS
368 when compared with PDB (Fig. 5A). These results support the idea that when a gene is
369 transcriptionally active in one media, the H3K27me3 levels are lower than H3K27me3
370 levels under less transcriptionally permissive growth. Integrating the transcriptional and
371 ChIP fold-changes for all genes between the media, we see that this association is true
372 for some, but not all genes that undergo transcriptional changes between the media (Fig.
373 5B). Globally, the distribution of H3K27me3 fold-changes per gene between media shows
374 that genes higher expressed in PDB have a significantly higher H3K27me3 fold-change
375 (i.e. less H3K27me3 in PDB growth), while MS higher expressed genes have a
376 significantly lower H3K27me3 fold-change (i.e. less H3K27me3 in MS growth) (Fig. 5B).
377 Results for PDB versus CZA growth showed that genes higher expressed in CZA
378 have higher H3K27me3 levels in PDB, consistent with the expected association (Fig. 5C).
379 For genes higher expressed in PDB however, we observed a higher H3K27me3 level in
380 PDB. Globally, the data indicated a lower H3K27me3 ChIP-signal for samples grown in
381 CZA (Fig. 5D, data shifted to left on x-axis). The integrated results indicated that genes
382 higher expressed in CZA had less H3K27me3 in CZA, but the PDB higher expressed
383 genes also had lower H3K27me3 in CZA. This difference, the overall lower H3K27me3
384 levels in CZA, may represent a biologically relevant difference between the growth
385 media, but may also reflect a technical bias encountered for ChIP using CZA grown
386 material. It is not possible to fully resolve these two possibilities with our current data.
387 Results for CZA versus MS growth showed that genes higher expressed in MS had
388 statistically similar levels of H3K27me3 ChIP-signal between the two media (Fig. 5E). For
389 genes higher expressed in CZA, there was significantly higher H3K27me3 ChIP-signal

390 during MS growth (Fig. 5E). The genome-wide integrated analysis, combining fold-
391 change between CZA and MS for transcription and H3K27me3 ChIP, showed that genes
392 more highly expressed in CZA indeed have significantly higher levels of H3K27me3 when
393 grown in MS (Fig. 5F). We again see the effect of the lower H3K27me3 ChIP-signal from
394 CZA-grown material, where the global fold-change values indicate higher levels of
395 H3M27me3 in MS-grown material overall (Fig. 5F). However, there is a clear group of
396 genes that are more highly expressed in MS medium that have an H3K27me3 fold-
397 change indicating a shift toward higher levels in CZA. This can be seen by the
398 significantly different marginal density plot for H3K27me3 fold-change, where the genes
399 higher expressed in MS have a significantly greater change towards higher H3K27me3
400 levels in CZA (Fig. 5F). Overall, the results show that in most comparisons, there is an
401 association between quantitative transcriptional levels and H3K27me3 signal, where
402 genes more highly expressed in a transcriptionally permissive media have less
403 H3K27me3 when compared to H3K27me3 levels in the repressive media. These results
404 are consistent with the observations of the qualitative H3K27me3 presence/absence
405 comparisons and suggests that H3K27me3 levels are generally stable, but can vary for
406 some genes in a quantitative manner to impact their transcription.

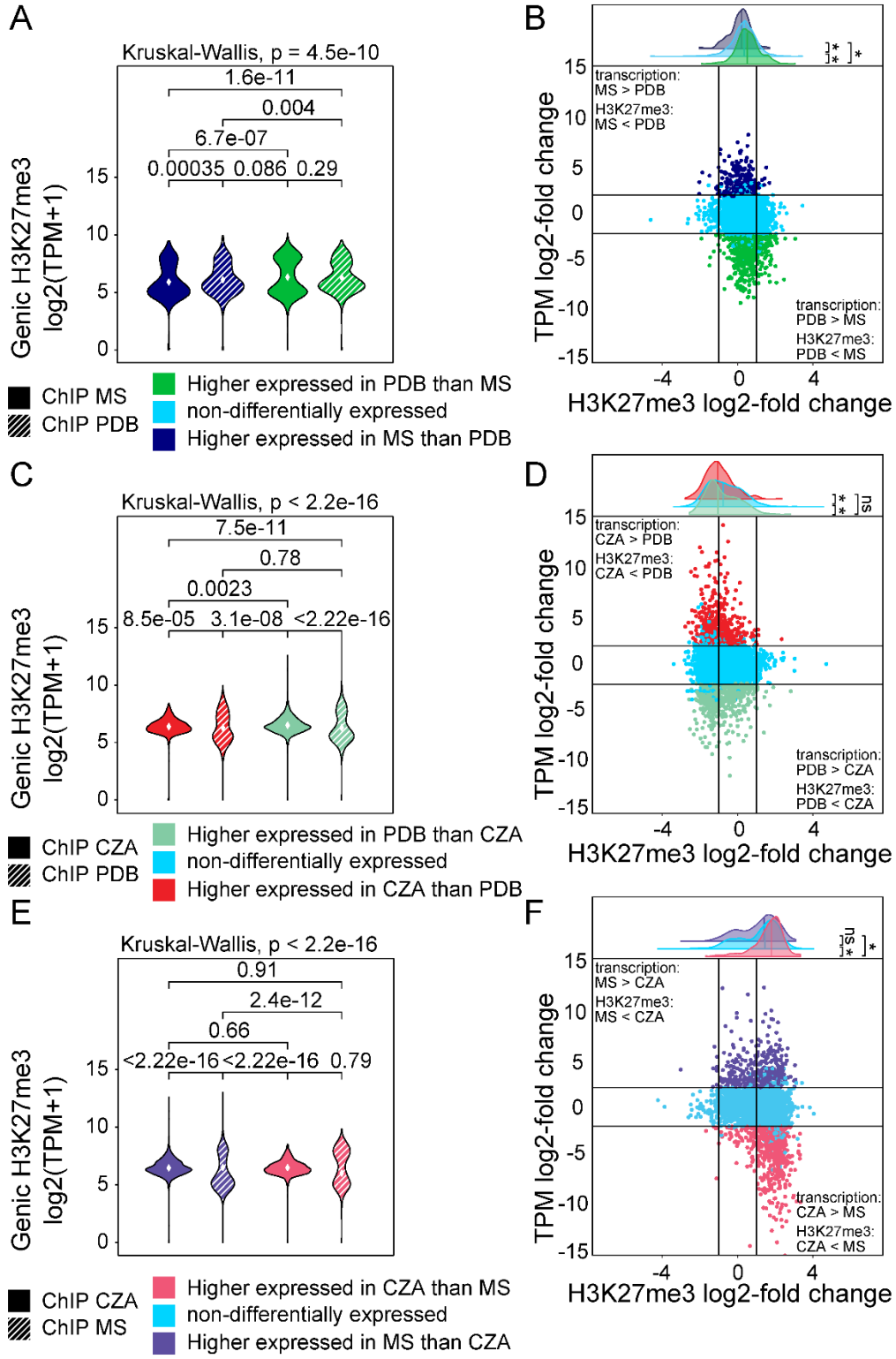

Figure 5. Differentially expressed genes associate with local changes in H3K27me3 coverage. Pairwise comparisons of differentially expressed genes for *V. dahliae* cultivated for 6 days in A,B) half-strength Murashige Skoog medium (MS) and Potato dextrose broth (PDB), C,D) Czapec-Dox (CZA) and PDB, and E,F) MS and CZA. A,C,E) H3K27me3 coverage over differentially expressed genes in each corresponding growth medium. Median values of violin plots are indicated with diamonds. B,D,F) per gene comparison of log2-fold change in transcription and genic H3K27me3 coverage. Black horizontal lines indicate TPM log_2-fold change of -2 and 2, black vertical lines indicate H3K27me3 log_2-fold change of -1 and 1. Significant difference of TPM values between growth media are determined with the One-Sample Wilcoxon Signed Rank Test and indicated by letters or by asterisks (*: $p \leq 0.05$).

418 **Genes induced *in planta* are largely H3K27me3 associated across all tested**
419 **growth conditions**

420 The presented analysis address histone modification and transcriptional dynamics
421 between axenic growth medium. A significant question is how do H3K27me3 levels
422 compare between more environmentally drastic growth conditions, such as *in vitro*
423 versus *in planta* growth. As we have thus far been unable to perform ChIP on *V. dahliae*
424 during host colonization due to a low pathogen-to-plant biomass, we assessed the *in*
425 *vitro* chromatin profiles for genes that are significantly induced during infection. First, we
426 grouped genes based on differential expression between PDB and *in planta* growth and
427 analysed the PDB grown chromatin profiles. We saw that genes higher expressed *in*
428 *planta* have significantly more H3K27me3 during PDB growth when compared with the
429 genes more highly expressed in PDB (Fig. 6A). These *in planta*-induced genes lacked
430 H3K4me2 and the DNA is less accessible during PDB growth, while genes highly
431 expressed in PDB are open and in active euchromatin (Fig. 6A). This pattern of *in planta*-
432 induced genes being highly H3K27me3-associated is also observed when analysed
433 relative to growth in MS and CZA (Fig. 6B,C).

434 To understand what genes are driving these differences, we investigated whether
435 *in planta*-induced genes that locate in H3K27me3 domains are overrepresented for genes
436 potentially involved in infection. There were approximately 1,000 genes more highly
437 expressed *in planta* when compared with any of the three media (Fig. 6D). We found
438 that, depending on the medium, from 36.5% to 53.4% of the *in planta*-induced genes
439 were located in H3K27me3 domains (Fig. 6D). We observed that the *in planta*-induced
440 genes within H3K27me3 domains have a higher, yet not statistically significant, fraction
441 of genes encoding secreted proteins or putative effectors when compared to all *in planta*
442 induced genes. Specifically, for genes in H3K27me3 domains that were *in planta*-induced
443 compared to PDB growth (376 genes total), 16.0% had a secretion signal and 5.1% were
444 predicted effectors. This is compared to all *in planta* induced genes relative to PDB (987
445 genes total), where 12.3% had a secretion signal and 3.2% were predicted effectors. For
446 CZA, 17.0% of the genes in H3K27me3 domains that were *in planta*-induced (418 genes

447 total) had a secretion signal and 5.7% were predicted effectors. This is compared to all *in*
448 *planta* induced genes relative to CZA (1,144 genes total), where 13.4% had a secretion
449 signal and 3.8% were predicted effectors. The results were similar for comparison to MS
450 grown samples. Thus, we consistently observed that *in planta*-induced genes in
451 H3K27me3 domains have a slightly higher fraction of genes that are potentially involved
452 in infection. Collectively, these results indicate that genes required for infection associate
453 with H3K27me3 and that chromatin dynamics are likely needed during *in planta* infection
454 to increase DNA accessibility concomitant with *in planta* transcription compared to the
455 measured state in PDB. Whether or not this activation is accompanied by loss or
456 dynamics of H3K27me3 levels will need to be directly assessed *in planta* in the future.

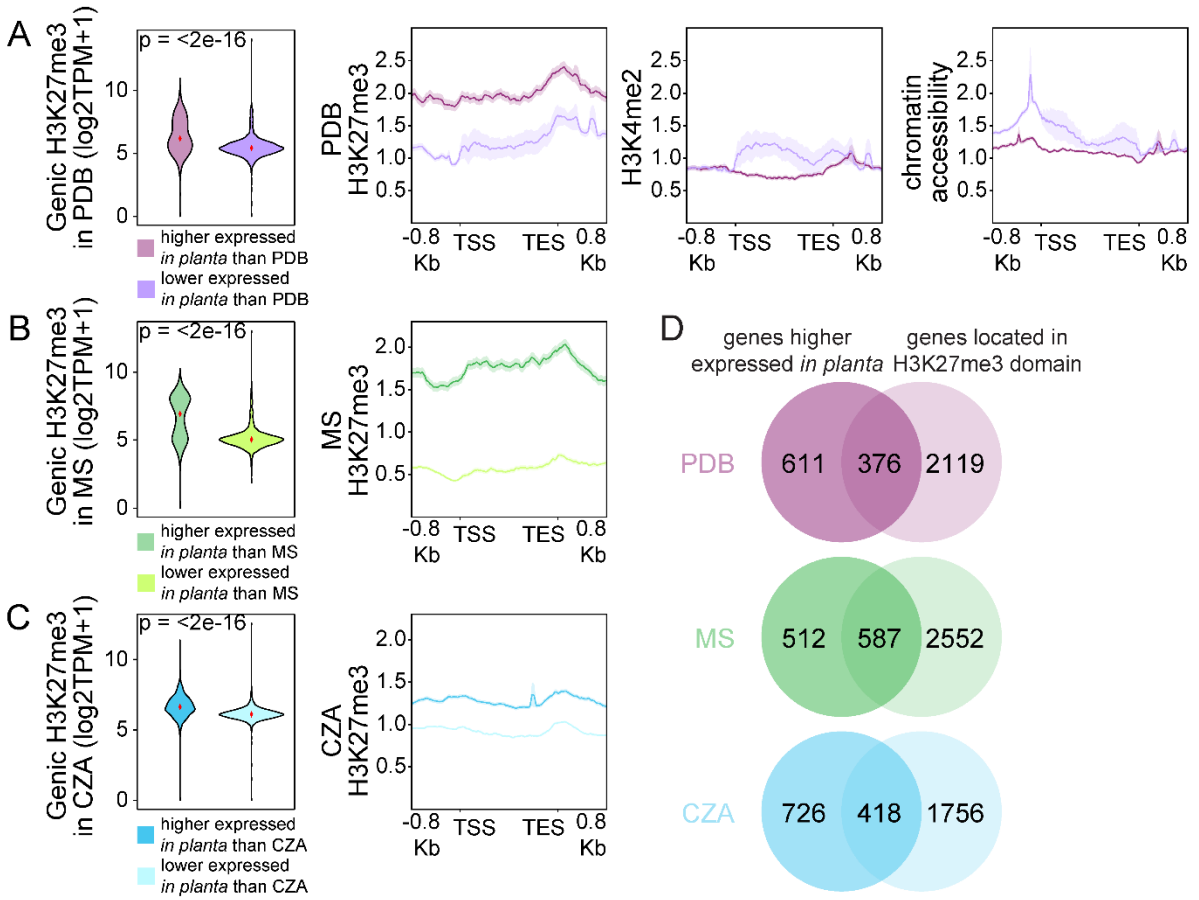

457

458 **Figure 6. *In planta*-induced genes are H3K27me3-associated under transcriptionally**
459 **repressive conditions.** Average coverage of chromatin features over genes differentially
460 expressed between in planta and A) 6 days of cultivation in Potato dextrose broth (PDB), B) half
461 strength Murashige Skoog medium (MS), and C) Czapec-Dox medium (CZA). D) overlap of genes
462 that are higher expressed *in planta* than in PDB, MS or CZA with genes located in an H3K27me3
463 domain in the corresponding growth medium. Significant differences of H3K27me3 coverage are
464 determined with the One-Sample Wilcoxon Signed Rank Test (*: p <= 0.05).

465 **DISCUSSION**

466 Chemical histone modifications play an essential role in transcriptional regulation, but
467 questions remain regarding their mechanism, especially in filamentous fungi. In our
468 study we show that many differentially transcribed genes between *in vitro* and *in planta*
469 growth are located in previously defined adaptive genomic regions (Cook *et al.*, 2020).
470 We report that a majority of the genes identified as being differentially transcribed
471 between the tested conditions reside in H3K27me3 domains. This mark only occupies
472 28.7% of the genes in the genome, but the rate of H3K27me3 association significantly
473 increases for differentially expressed genes by 35% to 70%.

474 Previous reports propose that H3K27me3 represses transcription of secondary
475 metabolite clusters in *Fusarium spp.* and *Epichloe festucae*, and effectors in
476 *Zymoseptoria tritici* and *Magnaporthe oryzae* (Connolly *et al.*, 2013; Chujo & Scott,
477 2014; Studt *et al.*, 2016; Möller *et al.*, 2019; Zhang *et al.*, 2021). However, these
478 reports have mainly relied on genomic association with H3K27me3, genetic perturbation
479 altering H3K27me3 deposition, and the analysis of only a few genes under natural
480 conditions. Given these previous findings, our hypothesis was that H3K27me3 levels are
481 dynamic during growth in different conditions and contribute to differential transcription.
482 We directly addressed this using genome-wide H3K27me3 profiling and RNA-seq under
483 different *in vitro* growth conditions. Consistent with reports in other fungi, we see that
484 H3K27me3 is associated with transcriptional repression, and that deleting *Set7*, encoding
485 the histone methyltransferase that is responsible for H3K27me3, led to induction of many
486 genes normally present in H3K27me3 domains. Importantly, our direct observations of
487 H3K27me3 levels and transcriptional output from three *in vitro* media showed that
488 H3K27me3 domains are generally stable globally. We see that 50% to 75% of the
489 identified H3K27me3 domains, depending on the medium analyzed, did not change
490 between the tested conditions. Despite many H3K27me3 domains not undergoing
491 presence/absence dynamics, numerous genes in these domains displayed differential
492 transcription between the tested conditions, indicating that complete loss of H3K27me3 is
493 not strictly required for transcriptional induction.

494 Even though our data suggest that qualitative H3K27me3 changes are not
495 sufficient to explain differential transcription under natural conditions alone, we do
496 provide empirical evidence that quantitative H3K27me3 dynamics are associated with
497 differentially expressed genes in *V. dahliae* grown under different *in vitro* conditions.
498 These results show that some genes grown in transcriptionally permissive media have a
499 lower H3K27me3 ChIP-signal when compared with growth in a transcriptionally
500 repressive media. We interpret these results as evidence for local, not global,
501 contribution of H3K27me3 quantitative dynamics to transcriptional regulation for these
502 genes. These results are consistent with data from *M. oryzae*, in which direct *in planta*
503 H3K27me3 ChIP-qPCR showed that some, but not all, analyzed regions displayed
504 differential H3K27me3 levels between *in planta* and *in vitro* conditions (Zhang *et al.*,
505 2021). We have not been able to directly assess histone modifications for *V. dahliae*
506 during plant infection, but we did analyze the *in vitro* growth H3K27me3 status of *in*
507 *planta*-induced genes. The identified *in planta*-induced genes have significantly higher
508 levels of H3K27me3 and the DNA is substantially less accessible compared to genes
509 highly expressed during *in vitro* growth. We conclude that dynamics for H3K27me3 can
510 contribute to differential gene expression under natural conditions, but it is not required,
511 and additional regulatory mechanisms are likely important to increase DNA accessibility
512 and enact transcription. An interesting finding in our research was the quantitative
513 association we observed between H3K27me3 levels and transcriptional output between
514 the growth conditions. This is interesting because it is not clear what mechanism explains
515 a quantitative rather than qualitative change in H3K27me3 levels. That is, a nucleosome
516 can have none, one, or two H3K27 tails with a tri-methyl modification, and quantitative
517 differences seen in our samples reflect either heterogeneity in H3K27me3 status for cells
518 in the population (e.g., 50% of cells are H3K27me3 and 50% are H3K27 non-modified)
519 or it represents bivalent chromatin domains (e.g., 100% of cells have 50% H3K27me3).
520 Bivalent domains are generally defined as DNA regions interacting with nucleosomes that
521 contain chemical modifications representative of both active and repressed chromatin,
522 with the prevailing example being the presence of both H3K4me3 and H3K27me3 (Blanco

523 *et al.*, 2020). Bivalent domains have been identified and described in animal systems,
524 and are thought to exist in a poised transcriptional state, with low steady state
525 transcription capable of rapid transcriptional activation during cellular differentiation
526 (Bernstein *et al.*, 2006; Voigt *et al.*, 2013). To our knowledge, bivalent domains have not
527 been formally described in fungi. Whether our data are the result of a heterogenous
528 population of cells or represent bivalent domains remains to be resolved. Nevertheless,
529 our results show that many genes differentially expressed between growth conditions are
530 associated with quantitative differences in H3K27me3 levels, providing evidence that
531 chemical histone modifications dynamics can play a transcriptional regulatory mechanism
532 in *V. dahliae*. As our experiments were based on differences between growth conditions,
533 these results may represent a general regulatory mechanism for environmentally
534 response genes.

535 At present, our conclusions are limited to the tested conditions, and it is possible
536 that analyzing H3K27me3 levels in different cell-types or growth stages (e.g. spores,
537 microsclerotia, *in planta* infection) may yield a different picture of global H3K27me3
538 distribution. Additionally, our experiments focused on steady-state growth on different
539 media as these provide a clear and reproducible transcriptional difference. It is possible
540 that H3K27me3 dynamics occur rapidly in response to environmental changes, cues, or
541 developmental stages that we did not capture.

542 It appears evident that H3K27me3 contributes to additional genome functions
543 beyond strict transcriptional repression, at least in fungi (Ridenour *et al.*, 2020). This is
544 supported by our data showing the a majority of H3K27me3 domains were stable
545 between the tested growth conditions, indicating these H3K27me3 domains have
546 additional functions. These stable H3K27me3 domains may represent another form of
547 constitutive heterochromatin, but this fact seems unlikely given that in our data many
548 stable H3K27me3 domains harbored differentially expressed genes between growth
549 media. Additionally, results in *N. crassa* have shown that genetic perturbation leading to
550 the genome-wide loss of H3K9me3 causes a redistribution of H3K27me3 to previously
551 H3K9me3 marked sites, but interestingly, this re-distribution does not result in

552 transcriptional silencing (Basenko *et al.*, 2015). Rather, the redistribution of H3K27me3
553 in *N. crassa* lacking H3K9me3 appears to contribute to genomic instability (Basenko *et*
554 *al.*, 2015; Lewis, 2017). In *Z. tritici*, the enrichment of H3K27me3 at dispensable
555 chromosomes and empirical evidence that H3K27me3 somehow increases genomic
556 instability, additionally supports the hypothesis that H3K27me3 contributes to additional
557 genomic functions beyond transcriptional regulation (Schotanus *et al.*, 2015; Möller *et*
558 *al.*, 2019). Additional research is needed to fully understand the mechanisms of
559 H3K27me3 targeting, dynamics, and impact on genome stability in fungi. The results
560 presented here show that H3K27me3 domains are largely similar between *in vitro* growth
561 conditions, but that quantitative differences in H3K27me3 levels are associated with
562 concomitant transcriptional differences between the tested conditions.

563 **MATERIALS AND METHODS**

564 **Fungal growth conditions**

565 *Verticillium dahliae* strain JR2 (CBS 143773; Faino et al., 2015) was cultured on potato
566 dextrose agar (PDA) (Oxoid, Thermo Scientific) at 22°C in the dark. Liquid cultures were
567 obtained by collecting conidiospores from PDA plates after approximately 2 weeks of
568 growth followed by inoculation at a final concentration of $1x10^4$ spores per mL into liquid
569 growth media. Media used in this study are potato dextrose broth (PDB) (Difco, Becton
570 Dickinson, Franklin Lakes, NJ, USA), half strength Murashige & Skoog plus vitamins (MS)
571 (Duchefa-Biochemie, Haarlem, The Netherlands) medium supplemented with 3%
572 sucrose, and Czapec-Dox medium (CZA) (Oxoid, Thermo Scientific, Waltham, MA, USA).
573 Liquid cultures were grown for 6 days in the dark at 22°C at 140 RPM. Mycelium was
574 collected by straining cultures through miracloth (22 µm) (EMD Millipore, Darmstadt,
575 Germany) and pressing to remove liquid after which the mycelium was flash frozen in
576 liquid nitrogen and ground to powder with a mortar and pestle. If required, samples were
577 stored at -20°C prior to nucleic acid extraction. All analyses were performed based on
578 triplicate cultures that were processed individually.

579

580 **RNA sequencing and analysis**

581 RNA was isolated from ground mycelium using TRIzol (Thermo Fisher Science, Waltham,
582 MA, USA) following manufacturer guidelines. Contaminating DNA was removed using the
583 TURBO DNA-free kit (Ambion, Thermo Fisher Science, Waltham, MA, USA) and RNA
584 integrity was assessed with gel-electrophoresis and quantified using a Nanodrop (Thermo
585 Fisher Science, Waltham, MA, USA). Library were prepared and singleend 50 bp
586 sequenced on the DNBseq platform at BGI (Hong Kong, China).

587 Sequencing reads were mapped to the reference annotation of *V. dahliae* strain
588 JR2 (Faino *et al.*, 2015) using Kallisto quant (Bray *et al.*, 2016) to calculate per gene TPM
589 values. Differential expression between cultivation in PDB and CZA, MS or during
590 colonization of *Arabidopsis thaliana* was determined using DESeq2 (Love *et al.*, 2014).

591 H3K27me3-enriched regions were determined using epic2 with a binsize of 2,500 bp
592 (Stovner & Sætrom, 2019).
593
594 **ChIP-sequencing and analysis**
595 ChIP-seq was performed as described previously (Cook et al., 2020). Frozen ground
596 mycelium was added to ChIP lysis buffer, dounced 40 times and subsequently sonicated
597 for 5 rounds of 20 seconds with 40 second rest stages on ice. Supernatants were
598 collected after centrifugation and treated with MNase (New England Biolabs, Ipswich, MA,
599 United States) for 10 minutes in a 37°C waterbath. MNase activity was quenched by
600 addition of EGTA and samples were subsequently pre-cleared by addition of 40 µl Protein
601 A Magnetic Beads (New England Biolabs, Ipswich, MA, United States) and rotating at 4°C
602 for 60 min. Beads were captured and supernatant was divided over new tubes containing
603 antibodies against either H3K4me2, H3K9me3 or H3K27me3 (ActiveMotif; #39913,
604 #39765 and #39155) and incubated overnight with continuous rotation at 4°C.
605 Subsequently, the antibodies were captured, washed and nucleosomes were eluted from
606 beads, after which DNA was treated with Proteinase-K and cleaned-up using chloroform.
607 DNA was isolated by overnight precipitation in ethanol and DNA concentration was
608 determined with the Qubit™ dsDNA HS Assay Kit (Thermo Fisher Science, Waltham, MA,
609 USA). Sequencing libraries were generated using the TruSeq ChIP Library Preparation Kit
610 (Illumina, San Diego, CA, United States) according to instructions, but without gel
611 purification and with use of the Velocity DNA Polymerase (BioLine, Luckenwalde,
612 Germany) for 25 cycles of amplification. Single-end 125bp sequencing was performed on
613 the Illumina HiSeq2500 platform at KeyGene N.V. (Wageningen, the Netherlands).
614 Raw reads were trimmed using TrimGalore (Martin, 2011) and mapped to the *V.*
615 *dahliae* strain JR2 reference genome (Faino *et al.*, 2015) using BWA-mem with default
616 settings (Li, 2013). Three regions of the genome were masked due to aberrant mapping,
617 (chr1:1-45000, chr2:3466000-3475000, chr3:1-4200). ATAC-seq reads of *V. dahliae*
618 cultured in PDB (Cook *et al.*, 2020) were treated similarly as ChIP-seq reads, but the
619 paired end read pairs were trimmed and mapped simultaneously, and only read-pairs

620 <100 bp were considered for further analyses, as these represent open DNA. Mapped
621 reads were RPGC-normalized using deepTools bamCoverage (Ramírez *et al.*, 2014) with
622 binsize 1,000 and smoothlength 3,000 for plotting over the genome, and binsize 10 and
623 smoothlength 30 for further analysis. Average coverage over gene bodies per expression
624 quintile was calculated using deepTools computeMatrix in scale-regions mode (Ramírez *et*
625 *al.*, 2014). Expression quintiles were generated by sorting all genes based on their
626 average TPM value from three replicates of *V. dahliae* cultured for 6 days in PDB. To
627 assess the presence of the histone marks over promoters (500 bp upstream of TSS) and
628 gene bodies (region between TSS and TES) of genes located in LS regions and the core
629 genome, we used deepTools multiBigwigSummary (Ramírez *et al.*, 2014) to calculate the
630 average coverage of the histone marks and chromatin accessibility for each gene.
631 Changes in H3K27me3 levels was determined by calculating the average coverage
632 over a gene using featureCounts (Liao *et al.*, 2014) on sorted bam files, and comparing
633 the coverage between duplicates of cultivation in PDB and CZA or MS with DESeq2 (Love
634 *et al.*, 2014). Changes in H3K27me3 and differential expression per gene were analysed.
635
636 **Generation of *Set7* deletion mutant**
637 The *Set7* deletion mutant (Δ*Set7*) was constructed as previously described (Santhanam,
638 2012). Briefly, genomic DNA regions flanking the 5′ and 3′ ends of the coding sequences
639 were amplified with PCR using primers listed in Table S1 (primers 1-4) and cloned in to
640 the pRF-HU2 vector (Frandsen *et al.*, 2008) using USER enzyme following the
641 manufacturer's protocol (New England Biolabs, MA, USA). Sequence-verified vectors were
642 transformed into *Agrobacterium tumefaciens* strain AGL1 and used for *V. dahliae*
643 conidiospore transformation as described previously (Santhanam, 2012). *V. dahliae*
644 transformants that appeared on hygromycin B were transferred to fresh PDA
645 supplemented with hygromycin B after five days. Putative transformants were screened
646 using PCR to verify deletion of the target gene sequence and integration of the selection
647 marker at the designated locus using primers listed in Table S1 (primers 5-8). Analysis

648 and comparison of gene expression in the *Set7* deletion mutant to type *V. dahliae* was
649 performed as described above.
650

651 **ACKNOWLEDGEMENTS**

652 This work was supported by a PhD grant of the Research Council Earth and Life Sciences
653 (project 831.15.002) to HMK, and by Human Frontier Science Program Postdoctoral
654 Fellowship (HFSP, LT000627/2014-L), by USDA's National Institute of Food and
655 Agriculture (award no. 2018-67013-28492) through the Plant Biotic Interactions
656 Program, and by the National Science Foundation (award no. 1936800) Division of
657 Molecular and Cellular Biosciences to DEC. Work in the laboratories of M.F.S and
658 B.P.H.J.T. is supported by the Research Council Earth and Life Sciences (ALW) of the
659 Netherlands Organization of Scientific Research (NWO). B.P.H.J.T acknowledges funding
660 by the Alexander von Humboldt Foundation in the framework of an Alexander von
661 Humboldt Professorship endowed by the German Federal Ministry of Education and
662 Research is furthermore supported by the Deutsche Forschungsgemeinschaft (DFG,
663 German Research Foundation) under Germany´s Excellence Strategy – EXC 2048/1 –
664 Project ID: 390686111. The authors declare no conflict of interest.

665 **REFERENCES**

666 **Aguilera J, Randez-Gil F, Prieto JA**. **2007**. Cold response in *Saccharomyces*
667 *cerevisiae*: new functions for old mechanisms. *FEMS Microbiology Reviews* **31**: 327–341.

668 **Bahn Y-S, Xue C, Idnurm A, Rutherford JC, Heitman J, Cardenas ME**. **2007**.
669 Sensing the environment: lessons from fungi. *Nature Reviews Microbiology* **5**: 57–69.

670 **Bannister AJ, Kouzarides T**. **2011**. Regulation of chromatin by histone modifications.
671 *Cell Research* **21**: 381–395.

672 **Basenko EY, Sasaki T, Ji L, Prybol CJ, Burckhardt RM, Schmitz RJ, Lewis ZA**.
673 **2015**. Genome-wide redistribution of H3K27me3 is linked to genotoxic stress and
674 defective growth. *Proceedings of the National Academy of Sciences* **112**: E6339–E6348.

675 **Bernstein BE, Mikkelsen TS, Xie X, Kamal M, Huebert DJ, Cuff J, Fry B, Meissner**
676 **A, Wernig M, Plath K**. **2006**. A bivalent chromatin structure marks key developmental
677 genes in embryonic stem cells. *Cell* **125**: 315–326.

678 **Blanco E, González-Ramírez M, Alcaine-Colet A, Aranda S, Di Croce L**. **2020**. The
679 bivalent genome: characterization, structure, and regulation. *Trends in Genetics* **36**:
680 118–131.

681 **Bray NL, Pimentel H, Melsted P, Pachter L**. **2016**. Near-optimal probabilistic RNA-seq
682 quantification. *Nature Biotechnology* **34**: 525–527.

683 **Buenrostro JD, Wu B, Chang HY, Greenleaf WJ**. **2015**. ATAC-seq: A method for
684 assaying chromatin accessibility genome-wide. *Current Protocols in Molecular Biology*
685 **2015**: doi: 10.1002/0471142727.mb2129s109.

686 **Chujo T, Scott B**. **2014**. Histone H3K9 and H3K27 methylation regulates fungal alkaloid
687 biosynthesis in a fungal endophyte-plant symbiosis. *Molecular Microbiology* **92**: 413–434.

688 **Connolly LR, Smith KM, Freitag M**. **2013**. The *Fusarium graminearum* histone H3 K27
689 methyltransferase KMT6 regulates development and expression of secondary metabolite
690 gene clusters. *PLoS Genetics* **9**: e1003916.

691 **Cook DE, Kramer HM, Torres DE, Seidl MF, Thomma BPHJ**. **2020**. A unique
692 chromatin profile defines adaptive genomic regions in a fungal plant pathogen. *eLife* **9**:
693 e62208.

694 **Depotter JRL, Shi-Kunne X, Missonnier H, Liu T, Faino L, Berg GCM, Wood TA,**
695 **Zhang B, Jacques A, Seidl MF, *et al.* 2019**. Dynamic virulence-related regions of the
696 plant pathogenic fungus *Verticillium dahliae* display enhanced sequence conservation.
697 *Molecular Ecology*: doi: 10.1111/mec.15168.
698 **Faino L, de Jonge R, Thomma BPHJ**. **2012**. The transcriptome of *Verticillium dahliae*-
699 infected *Nicotiana benthamiana* determined by deep RNA sequencing. *Plant Signaling &*
700 *Behavior* **7**: 1065–1069.
701 **Faino L, Seidl M, Datema E, van den Berg GCM, Janssen A, Wittenberg AHJ,**
702 **Thomma BPHJ**. **2015**. Single-molecule real-time sequencing combined with optical
703 mapping yields completely finished fungal genome. *mBio* **6**: e00936–15.
704 **Faino L, Seidl MF, Shi-Kunne X, Pauper M, Van Den Berg GCM, Wittenberg AHJ,**
705 **Thomma BPHJ**. **2016**. Transposons passively and actively contribute to evolution of the
706 two-speed genome of a fungal pathogen. *Genome Research* **26**: 1091–1100.
707 **Fan A, Mi W, Liu Z, Zeng G, Zhang P, Hu Y, Fang W, Yin W-B**. **2017**. Deletion of a
708 histone acetyltransferase leads to the pleiotropic activation of natural products in
709 Metarhizium robertsii. *Organic Letters* **19**: 1686–1689.
710 **Fradin EF, Thomma BPHJ**. **2006**. Physiology and molecular aspects of Verticillium wilt
711 diseases caused by *V. dahliae* and *V. albo-atrum*. *Molecular Plant Pathology* **7**: 71–86.
712 **Frandsen RJN, Andersson JA, Kristensen MB, Giese H**. **2008**. Efficient four
713 fragment cloning for the construction of vectors for targeted gene replacement in
714 filamentous fungi. *BMC Molecular Biology* **9**: 70.
715 **Freitag M**. **2017**. Histone Methylation by SET Domain Proteins in Fungi. *Annual Review*
716 *of Microbiology* **71**: 413–439.
717 **Galazka JM, Freitag M**. **2014**. Variability of chromosome structure in pathogenic fungi-
718 of 'ends and odds'. *Current Opinion in Microbiology* **20**: 19–26.
719 **Gibson G**. **2008**. The environmental contribution to gene expression profiles. *Nature*
720 *Reviews Genetics* **9**: 575–581.

721 **Heijmans BT, Tobi EW, Stein AD, Putter H, Blauw GJ, Susser ES, Slagboom PE,**
722 **Lumey LH**. **2008**. Persistent epigenetic differences associated with prenatal exposure to
723 famine in humans. *Proceedings of the National Academy of Sciences* **105**: 17046–17049.
724 **Herrera CM, Pozo MI, Bazaga P**. **2012**. Jack of all nectars, master of most: DNA
725 methylation and the epigenetic basis of niche width in a flower-living yeast. *Molecular*
726 *Ecology* **21**: 2602–2616.
727 **Jamieson K, Rountree MR, Lewis Z a, Stajich JE, Selker EU**. **2013**. Regional control
728 of histone H3 lysine 27 methylation in *Neurospora*. *Proceedings of the National Academy*
729 *of Sciences of the United States of America* **110**: 6027–32.
730 **De Jonge R, Bolton MD, Kombrink A, van den Berg GCM, Yadeta KA, Thomma**
731 **BPHJ**. **2013**. Extensive chromosomal reshuffling drives evolution of virulence in an
732 asexual pathogen. *Genome Research* **23**: 1271–1282.
733 **Kim J-M, Sasaki T, Ueda M, Sako K, Seki M**. **2015**. Chromatin changes in response to
734 drought, salinity, heat, and cold stresses in plants. *Frontiers in Plant Science* **6**: doi:
735 10.3389/fpls.2015.00114.
736 **Klosterman SJ, Subbarao K V., Kang S, Veronese P, Gold SE, Thomma BPHJ,**
737 **Chen Z, Henrissat B, Lee YH, Park J, *et al.* 2011**. Comparative genomics yields
738 insights into niche adaptation of plant vascular wilt pathogens. *PLoS Pathogens* **7**:
739 e1002137.
740 **Kronholm I, Johannesson H, Ketola T**. **2016**. Epigenetic control of phenotypic
741 plasticity in the filamentous fungus *Neurospora crassa*. *G3: Genes, Genomes, Genetics* **6**:
742 4009–4022.
743 **Lewis ZA**. **2017**. Polycomb group systems in fungi: new models for understanding
744 polycomb repressive complex 2. *Trends in Genetics* **33**: 220–231.
745 **Lewis ZA, Adhvaryu KK, Honda S, Shiver AL, Knip M, Sack R, Selker EU**. **2010**.
746 DNA methylation and normal chromosome behavior in *Neurospora* depend on five
747 components of a histone methyltransferase complex, DCDC. *PLoS Genet* **6**: e1001196.

748 **Lewis ZA, Honda S, Khlafallah TK, Jeffress JK, Freitag M, Mohn F, Schübeler D,**
749 **Selker EU**. **2009**. Relics of repeat-induced point mutation direct heterochromatin
750 formation in *Neurospora crassa*. *Genome Research* **19**: 427–437.
751 **Li H**. **2013**. Aligning sequence reads, clone sequences and assembly contigs with BWA-
752 MEM. *arXiv:1303.3997*.
753 **Liao Y, Smyth GK, Shi W**. **2014**. featureCounts: an efficient general purpose program
754 for assigning sequence reads to genomic features. *Bioinformatics* **30**: 923–930.
755 **Love MI, Huber W, Anders S**. **2014**. Moderated estimation of fold change and
756 dispersion for RNA-seq data with DESeq2. *Genome Biology* **15**: 550.
757 **Martin M**. **2011**. Cutadapt removes adapter sequences from high-throughput
758 sequencing reads. *EMBnet Journal* **17**: 10–12.
759 **Martin EM, Fry RC**. **2018**. Environmental influences on the epigenome: exposure-
760 associated DNA methylation in human populations. *Annual review of public health* **39**:
761 309–333.
762 **Möller M, Schotanus K, Soyer JL, Haueisen J, Happ K, Stralucke M, Happel P,**
763 **Smith KM, Connolly LR, Freitag M, *et al.* 2019**. Destabilization of chromosome
764 structure by histone H3 lysine 27 methylation. *PLoS Genetics* **15**: e1008093.
765 **Ramírez F, Dündar F, Diehl S, Grüning BA, Manke T**. **2014**. deepTools: a flexible
766 platform for exploring deep-sequencing data. *Nucleic Acids Research* **42**: W187–W191.
767 **Reyes-Dominguez Y, Boedi S, Sulyok M, Wiesenberger G, Stoppacher N, Krska R,**
768 **Strauss J**. **2012**. Heterochromatin influences the secondary metabolite profile in the
769 plant pathogen *Fusarium graminearum*. *Fungal Genetics and Biology* **49**: 39–47.
770 **Reyes-Dominguez Y, Bok JW, Berger H, Shwab EK, Basheer A, Gallmetzer A,**
771 **Scazzocchio C, Keller N, Strauss J**. **2010**. Heterochromatic marks are associated with
772 the repression of secondary metabolism clusters in *Aspergillus nidulans*. *Molecular*
773 *Microbiology* **76**: 1376–1386.
774 **Ridenour JB, Möller M, Freitag M**. **2020**. Polycomb repression without bristles:
775 facultative heterochromatin and genome stability in fungi. *Genes* **11**: 638.

776 **Santhanam P**. **2012**. Random insertional mutagenesis in fungal genomes to identify
777 virulence factors. In: Plant Fungal Pathogens. Springer, 509–517.
778 **Schmit JP, Mueller GM**. **2007**. An estimate of the lower limit of global fungal diversity.
779 *Biodiversity and Conservation* **16**: 99–111.
780 **Schneper L, Düvel K, Broach JR**. **2004**. Sense and sensibility: nutritional response
781 and signal integration in yeast. *Current Opinion in Microbiology* **7**: 624–630.
782 **Schotanus K, Soyer JL, Connolly LR, Grandaubert J, Happel P, Smith KM, Freitag**
783 **M, Stukenbrock EH**. **2015**. Histone modifications rather than the novel regional
784 centromeres of Zymoseptoria tritici distinguish core and accessory chromosomes.
785 *Epigenetics & Chromatin* **8**: 41.
786 **Seidl MF, Cook DE, Thomma BPHJ**. **2016**. Chromatin biology impacts adaptive
787 evolution of filamentous plant pathogens. *PLoS Pathogens* **12**: e1005920.
788 **Seidl MF, Kramer HM, Cook DE, Lorencini Fiorin G, van den Berg GCM, Faino L,**
789 **Thomma BPHJ**. **2020**. Repetitive elements contribute to the diversity and evolution of
790 centromeres in the fungal genus *Verticillium*. *mBio*: doi: 10.1128/mBio.01714–20.
791 **Selvig K, Alspaugh JA**. **2011**. pH response pathways in fungi: adapting to host-derived
792 and environmental signals. *Mycobiology* **39**: 249–256.
793 **Shi-Kunne X, Faino L, van den Berg GCM, Thomma BPHJ, Seidl MF**. **2018**.
794 Evolution within the fungal genus *Verticillium* is characterized by chromosomal
795 rearrangement and gene loss. *Environmental Microbiology* **20**: 1362–1373.
796 **Slepecky RA, Starmer WT**. **2009**. Phenotypic plasticity in fungi: a review with
797 observations on *Aureobasidium pullulans*. *Mycologia* **101**: 823–832.
798 **Slotkin RK, Martienssen R**. **2007**. Transposable elements and the epigenetic
799 regulation of the genome. *Nature Reviews Genetics* **8**: 272–285.
800 **Soyer JL, El Ghalid M, Glaser N, Ollivier B, Linglin J, Grandaubert J, Balesdent**
801 **MH, Connolly LR, Freitag M, Rouxel T, *et al.* 2014**. Epigenetic control of effector
802 gene expression in the plant pathogenic fungus *Leptosphaeria maculans*. *PLoS Genetics*
803 **10**: e1004227.

804 **Soyer JL, Möller M, Schotanus K, Connolly LR, Galazka JM, Freitag M,**
805 **Stukenbrock EH**. **2015**. Chromatin analyses of *Zymoseptoria tritici*: methods for
806 chromatin immunoprecipitation followed by high-throughput sequencing (ChIP-seq).
807 *Fungal Genetics and Biology* **79**: 63–70.
808 **Stovner EB, Sætrom P**. **2019**. epic2 efficiently finds diffuse domains in ChIP-seq data.
809 *Bioinformatics* **35**: 4392–4393.
810 **Studt L, Rösler SM, Burkhardt I, Arndt B, Freitag M, Humpf HU, Dickschat JS,**
811 **Tudzynski B**. **2016**. Knock-down of the methyltransferase Kmt6 relieves H3K27me3
812 and results in induction of cryptic and otherwise silent secondary metabolite gene
813 clusters in *Fusarium fujikuroi*. *Environmental Microbiology* **18**: 4037–4054.
814 **Tian L, Chen ZJ**. **2001**. Blocking histone deacetylation in *Arabidopsis* induces pleiotropic
815 effects on plant gene regulation and development. *Proceedings of the National Academy*
816 *of Sciences* **98**: 200–205.
817 **Trojer P, Reinberg D**. **2007**. Facultative heterochromatin: is there a distinctive
818 molecular signature? *Molecular Cell* **28**: 1–13.
819 **Voigt P, Tee W-W, Reinberg D**. **2013**. A double take on bivalent promoters. *Genes &*
820 *development* **27**: 1318–1338.
821 **Wang J, Jia ST, Jia S**. **2016**. New insights into the regulation of heterochromatin.
822 *Trends in Genetics* **32**: 284–294.
823 **Wiemann P, Sieber CMK, von Bargen KW, Studt L, Niehaus EM, Espino JJ, Huß K,**
824 **Michielse CB, Albermann S, Wagner D, *et al.* 2013**. Deciphering the cryptic genome:
825 genome-wide analyses of the rice pathogen *Fusarium fujikuroi* reveal complex regulation
826 of secondary metabolism and novel metabolites. *PLoS Pathogens* **9**: e1003475.
827 **Zannas AS, Arloth J, Carrillo-Roa T, Iurato S, Röh S, Ressler KJ, Nemeroff CB,**
828 **Smith AK, Bradley B, Heim C**. **2015**. Lifetime stress accelerates epigenetic aging in an
829 urban, African American cohort: relevance of glucocorticoid signaling. *Genome biology*
830 **16**: 1–12.

831 **Zhang W, Huang J, Cook DE**. **2021**. Histone modification dynamics at H3K27 are
832 associated with altered transcription of in planta induced genes in *Magnaporthe oryzae*.
833 *PLoS genetics* **17**: e1009376.

834 **FIGURE LEGENDS**

835 **Figure 1. Genes that are higher expressed in CZA, MS and *in planta* than in PDB**
836 **are overrepresented in adaptive genomic regions and in H3K27me3 domains.**
837 Fractions of total genes and genes that are higher expressed than in PDB that locate in
838 (A) adaptive genomic regions and (B) H3K27me3-enriched regions. Increased expression
839 is determined between six days of cultivation *in vitro* of *V. dahliae* in potato dextrose
840 broth (PDB) and 6 days of cultivation in Czapec-Dox (CZA) and half-strength Murashige
841 Skoog medium (MS), and infection of *Arabidopsis thaliana* (21 dpi) (*in planta*). Fractions
842 of higher expressed genes that reside in adaptive genomic regions or H3K27me3-
843 enriched regions are reported for log2-fold changes >1, 2, 3, 4, 5, 6 and 7, respectively.
844 H3K27me3-enrichment was determined for *V. dahliae* cultivation during six days in PDB.
845 Black numbers above the bars indicate numbers of genes per gene set. White numbers at
846 bottom of the bars indicate the numbers of genes that locate in adaptive genomic or
847 H3K27me3-domain per gene set. Significance of fraction differences was calculated for
848 each fraction of higher expressed genes in adaptive genomic regions when compared
849 with the fraction of total genes in adaptive genomic regions, by the two-sided two-
850 proportions Z-test (*: $p \leq 0.05$).

851

852 **Figure 2. Lowly and non-expressed genes associate with H3K27me3.** A) Whole
853 genome distribution of the euchromatin-associated histone modification H3K4me2, the
854 constitutive heterochromatin-associated histone modification H3K9me3, the facultative
855 heterochromatin-associated histone modification H3K27me3 and chromatin accessibility
856 as determined by ATAC-seq, based on chromosome 5 as an example. Genes are
857 indicated in light blue, transposons are indicated in red, centromere is indicated in dark
858 blue and adaptive genomic regions are indicated in yellow. B,C) Relative coverage of
859 chromatin accessibility and the histone marks H3K4me2, H3K9me3, H3K27me3 over
860 gene bodies (between transcription start site (TSS) and transcription end site (TES))
861 ±800 bp of flanking sequence, grouped into quintiles based on gene expression levels

862 upon cultivation for six days potato dextrose broth (PDB), for (B) all genes, and for (C)
863 all H3K27me3-enriched genes.
864
865 **Figure 3. Genetic perturbation of H3K27me3 results in induction of genes that**
866 **are transcriptionally regulated in different growth conditions.** A) Fractions of
867 induced (log2 fold change >1, p<0.05) and repressed (log2 fold change <-1, p<0.05)
868 genes and genes that are not differentially expressed between wild-type and ΔSet7 that
869 (B) locate in H3K27me3 domains and (C-E) are higher expressed in CZA, MS and *in*
870 *planta* than in PDB.
871
872 **Figure 4. Differential H3K27 methylation partially explains differential**
873 **expression.** A) The number of genes located in H3K27me3 domains for *V. dahliae*
874 cultivated for 6 days in Czapec-Dox (CZA), half-strength Murashige Skoog medium (MS)
875 and Potato dextrose broth (PDB). B) Transcriptional values from RNA-seq, represented as
876 TPM values in each growth medium. The genes were grouped between those consistently
877 localized in H3K27me3 domains (1631 genes) and genes not present in H3K27me3
878 domains. C,D) Transcription TPM values in each growth medium for genes in H3K27me3
879 domains found in C) two or D) one of three tested *in vitro* growth media. Median values
880 of violin plots are indicated with diamonds. Significant difference of TPM values between
881 growth media are determined with the One-Sample Wilcoxon Signed Rank Test (*: p <=
882 0.05).
883
884 **Figure 5. Differentially expressed genes associate with local changes in**
885 **H3K27me3 coverage.** Pairwise comparisons of differentially expressed genes for *V.*
886 *dahliae* cultivated for 6 days in A,B) half-strength Murashige Skoog medium (MS) and
887 Potato dextrose broth (PDB), C,D) Czapec-Dox (CZA) and PDB, and E,F) MS and CZA.
888 A,C,E) H3K27me3 coverage over differentially expressed genes in each corresponding
889 growth medium. Median values of violin plots are indicated with diamonds. B,D,F) per
890 gene comparison of log2-fold change in transcription and genic H3K27me3 coverage.

891 Black horizontal lines indicate TPM log_2-fold change of -2 and 2, black vertical lines
892 indicate H3K27me3 log_2-fold change of -1 and 1. Significant difference of TPM values
893 between growth media are determined with the One-Sample Wilcoxon Signed Rank Test
894 and indicated by letters or by asterisks (*: $p \leq 0.05$).
895
896 **Figure 6. *In planta*-induced genes are H3K27me3-associated under**
897 **transcriptionally repressive conditions.** Average coverage of chromatin features over
898 genes differentially expressed between in planta and A) 6 days of cultivation in Potato
899 dextrose broth (PDB), B) half strength Murashige Skoog medium (MS), and C) Czapec-
900 Dox medium (CZA). D) overlap of genes that are higher expressed *in planta* than in PDB,
901 MS or CZA with genes located in an H3K27me3 domain in the corresponding growth
902 medium. Significant differences of H3K27me3 coverage are determined with the One-
903 Sample Wilcoxon Signed Rank Test (*: $p <= 0.05$).

904 **ADDITIONAL FILES**

905 **Fig. S1. Distribution of chromatin features over all chromosomes.** Whole genome
906 distribution of the euchromatin-associated histone modification H3K4me2 (green line),
907 the constitutive heterochromatin-associated histone modification H3K9me3 (red line), the
908 facultative heterochromatin-associated histone modification H3K27me3 (yellow line) and
909 chromatin accessibility (blue line) as determined by ATAC-seq. Genes are indicated in
910 light blue, transposons are indicated in red, centromere is indicated in dark blue and
911 adaptive genomic regions are indicated in yellow.

912 **Fig. S2. Gene expression correlates with histone modification presence and**
913 **chromatin accessibility.** RPGC normalized coverage of the histone marks H3K4me2,
914 H3K9me3, H3K27me3 and chromatin accessibility over gene bodies (between
915 transcription start site (TSS) and transcription end site (TES)) ±800 bp of flanking
916 sequence. Each row represents a single gene, and are sorted based on their TPM value
917 upon cultivation for six days potato dextrose broth (PDB), with the top gene being most
918 highly expressed. Genes are grouped in expression quintiles as in Figure 3A.

919 **Fig. S3. The *V. dahliae ΔSet7* deletion mutant loses H3K27me3.** Histone isolations
920 of wild-type, *ΔDim2*, *ΔDim5*, *ΔHP1* and *ΔSet7* were tested for presence of the H3K27me3
921 histone modification by Western blot. Antibody against H3 was used as loading control.

922 **Fig. S4. Genes associated with H3K27me3 in wild type *V. dahliae* are stronger**
923 **transcriptionally induced in the *ΔSet7* mutant than genes that are not**
924 **associated with H3K27me3.** Log2-fold change of expression between wild type and
925 *ΔSet7* mutant for genes associated with H3K27me3 in wild type (green) and those not
926 associated with H3K27me3 in wild type (red). Significant difference of log2-fold change
927 between gene sets are determined with the One-Sample Wilcoxon Signed Rank Test (*:
928 $p <= 0.05$).

929 **Fig. S5. Distribution of H3K27me3 for *V. dahliae* cultivated in *in vitro* growth**
930 **media.** Replicates of *V. dahliae* cultivated for 6 days in Potato dextrose broth (PDB), half

931 strength Murashige Skoog medium (MS) and Czapec-Dox medium (CZA). A) Distribution
932 of H3K27me3 over the *V. dahliae* genome, predicted H3K27me3 domains are indicated
933 as blocks below each H3K27me3 track. Adaptive genomic regions are highlighted in
934 yellow. B) Distribution of H3K27me3 over chromosome 5 of *V. dahliae*. Genomic regions
935 within H3K27me3 domains that are visibly different between growth conditions are
936 highlighted in grey.

937 **Table S1.** Primers used to delete and analyse the *Set7* coding sequence in *V. dahliae*.